Research Article

Ultrasonic testing system design for defect visualization of inhomogeneous multi-layered pipes

Ye Zhu[1] · Yi Liang[1] · Shicheng Wei[1] · Yujiang Wang[1] · Bo Wang[1]

Received: 24 July 2019 / Accepted: 31 October 2019 / Published online: 9 November 2019

Abstract
One of the major concerns of pipe equipment used for oil, gas and nuclear power generation, is their failure due to corrosion and abrasion of their inner walls. However, current methods have some problems detecting the inner wall of long and deep pipes, which has become an urgent safety problem. In this paper, we have designed and tested a suitable scanning and imaging method that offers high quality imaging, high efficiency and low cost. We applied the technique on remanufactured ceramic-lined steel composite pipe parts using a 4-module visualization nondestructive testing device. Digital signal and imaging algorithms were employed to superimpose multi-interface images to reconstruct 3D models of tested pipes with defects. Our findings suggest that ultrasonic scanning technique is feasible to analyze inner wall damages. The newly-designed hardware and software system shows efficiency and effectivity in the testing experiments on specimens with artificial markers and defects.

Keywords Inhomogeneous multi-layered pipes · Ultrasonic nondestructive testing (UT) · Signal processing algorithm · Image superposition

1 Introduction

Long and deep pipes (the aspect ratio > 10) with thermal and mechanical properties are playing a significant role in a variety of fields including oil and gas exploration, nuclear power generation, etc. Their widespread applicability and large consumption have resulted in huge quantities of metal scraps. In recent years, a reliable remanufacturing method has been applied on discarded oil pipes. The method is basically to synthesize a ceramic coating on the inner wall via self-propagation high-temperature synthesis (SHS) technology to abtain anti-corrosion and wear-resistance properties, thus turning the waste into new products.

In oil industry, it is usually difficult to produce and inspect composite pipes with a high aspect ratio. For example, a specified oil extraction pipe is 9.6 m in length, while its external diameter is only 73 mm, which makes the aspect ratio more than 100. Therefore, inner wall inspection has become an obstacle in both industrial production and actual service.

The remanufacturing industry is still developing. At present, there are two main NDT methods used in remanufacturing production processes of deep and long composite pipe parts, i.e., the magnetic flux leakage method and the manual endoscope inspection method. Before remanufacturing processes, the former can be used to select waste steel tubes of which the residual thickness is within an accepted range in spite of corrosion-induced reduction of the wall. Those meeting the thickness requirement will be considered for subsequent remanufacturing processes. However, a main limitation of this method is that it is more sensitive to surface and near surface defects rather than interior ones. After the remanufacturing process, workers can perform manually the endoscopic detection to inspect

✉ Yi Liang, liangyi365@126.com | [1]National Key Laboratory for Remanufacturing, Academy of Army Armored Forces, Beijing 100072, China.

the inner wall of the remanufactured deep hole with naked eyes, which is time-consuming and resource-wasting. Besides the remanufacturing industry, internal rotating inspection systems (IRIS) with an immersion ultrasonic probe or an underground camera have been developed to get higher accuracy and efficiency for pipe inspection in many application fields. The wide range of tested material types and pipe diameters makes IRIS a promising method of inspecting long and deep composite pipes. However, the limitation exists in the situation where testing facilities hardly have access to the inside of the pipes. Phased array ultrasonic testing (PAUT) is a high-efficiency method which is also a prospective candidate for different material types especially for tested objects with complicated geometries, while the imaging still requires improvement of visualization.

Many researchers have successfully employed ultrasonic C-scan methods on multi-layered materials. The research group of Skjelvareid et al. [1, 2] used an exterior rotating transducer instead of an interior one on small diameter pipes. They have been working on the synthetic aperture focusing technique (SAFT) for immersion testing of the water-PMMA-Al structure and simulations of cylindrical objects with multiple homogeneous layers. Kolkoori et al. [3] evaluated ultrasonic C-scan images quantitatively in homogeneous layered materials using a 3D ray tracing model. Iyer et al. [4] conducted A-, B- and C-scan on concrete pipes and captured images of different kinds of defects. Yang et al. [5] presented an efficient motion trajectory method for ultrasonic image reconstruction. Based on that, Cui et al. [6] developed a novel scan-conversion algorithm of line segment which further accelerated the accurate calculation of point of incidence (POI) in a double-layer object. These studies mainly use water immersion coupling method requiring a large water tank to immerse test objects, which limits the application possibilities. Meanwhile, the material in each layer of the studied objects is homogeneous. It follows that materials with multiple inhomogeneous layers in service are rarely examined with ultrasonic scanning methods and there are few effective means of onsite monitoring for them, considering characteristics of the actual service environment.

Our research focuses on eliminating limitations on both materials and detecting processes. An ultrasonic visualization NDT system is developed for pipes of a high aspect ratio, which has the potential to be applied in many occasions and to solve the aforesaid problems. Instead of testing from inside the pipe where it is not always accessible for testing facilities, the newly designed system realizes testing from outside the pipe. This enables in-service pipeline to be inspected on site. We also avoid using cumbersome water immersion containers in the whole inspection system. The mechanical module with rotating units

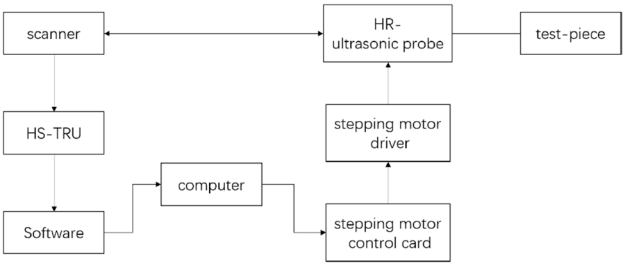

Fig. 1 A schematic of the experimental setup

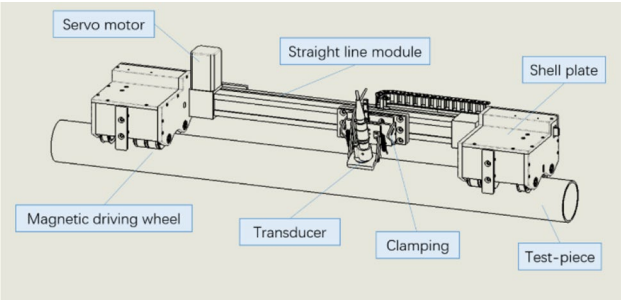

Fig. 2 The design sketch of the experimental setup

makes it easier to move automatically around the outer surface of the tested pipes, Pipe parts with an inhomogeneous ceramic layer resulting from the centrifugal effect during the manufacturing process are taken as the main study object. Signal processing and imaging algorithms containing image superposition method produce institutive reconstructed 3D images of defective multi-layered objects. By introducing new designing concepts of both hardware and software for composite pipe inspection, the new system raises the accuracy and practicability in testing processes, which is expected to provide theoretical basis and technical support for the quality control procedure of pipe products.

2 Experiments

2.1 Experimental setup

A schematic of the proposed experimental setup is shown in Fig. 1, with a design sketch in Fig. 2 and a photo of the real setup in Fig. 3. It is composed of four modules, namely the ultrasonic measurement module, the mechanical motion module, the electrical control module and the coupling/auxiliary module.

The ultrasonic measurement module is used for data collection, image processing and quantitative analysis. Different from traditional imaging method, data at multiple

Fig. 3 A photo of the real device

interfaces are superimposed. That means, two C-scan images are generated at the interfaces, namely the echo wave of the metal-ceramic joint and the echo wave of the ceramic layer respectively. The two images are superimposed so that the defects at the metal-ceramic interface and the ceramic layer are displayed on one C-scan image at the same time.

Data acquisition is completed jointly by the ultrasonic transmission/reception device and the synchronous/servo motor. An ultrasonic pulse transmission/reception device is adopted, which contains a high-speed A/D (80 MHz) converter [7]. Ultrasonic data are acquired by the pulse-echo method, using the square wave with an amplitude of 230 V and a duty cycle of 50%. A flat single crystal transducer for water immersion is employed, with a diameter of 0.5 in. and a resonance frequency of 5 Hz. The pulse duration (PD) is adjusted to the half of the TOF (time-of-flight) according to the following formula [8, 9]:

$$\begin{cases} c_{aver.} = \dfrac{2d}{\frac{2d_1}{c_1} + \frac{2d_2}{c_2} + \frac{2d_3}{c_3} + \frac{2d_4}{c_4}} = \dfrac{dc_1c_2c_3c_4}{d_1c_2c_3c_4 + d_2c_1c_3c_4 + d_3c_1c_2c_4 + d_4c_1c_2c_3} \\ PD = \dfrac{d}{2c_{aver.}} \end{cases}$$

where d is the aggregate thickness of the composite pipe wall. d_1, d_2, d_3, d_4 and c_1, c_2, c_3, c_4 are the thicknesses and longitudinal sound velocities respectively of the four layers from the outer to the inner.

After the industrial personal computer (IPC) collects ultrasound data, wavelet and threshold functions are applied for noise reduction and image segmentation. After denoising and defect feature extraction, ultrasonic echo signal reconstruction images can be acquired by MATLAB functions of signal processing algorithms including surface interplating fitting, image superposition and area proportion calculation, etc., thus to make further qualitative and quantitative characterization of defects, including parameters of the defect size, depth, shape and distribution.

The mechanical motion module includes scanning device, transducer and its clamping device, as well as magnetic adsorption device. The scanning resolution accuracy can be adjusted to realize 3D imaging. The resolution accuracy is theoretically 0.5 × 0.5 mm, which means the actual detected diameter of the device can be slightly larger than 0.5 mm considering some errors. The traction device uses a large torque stepper motor and magnetic driving wheels driven by it. The surface of the magnetic wheels is coated with skidproof rubber to provide enough adhesion force for rotating adsorption, which enables the device to be adsorbed on the pipe and to fulfil rotating walking measurement. The transducer clamping device is fixed on the linear module and moves synchronously with the synchronous belt in the module. A cardan joint-type transducer holder and a protective steel sleeve are adopted. Through the joint action of the coupling device and the spring mechanism, the transducer orientation can be automatically adjusted, so that the transducer always contacts the outer wall of the pipe along the normal direction and keeps the direction of the sound beam always perpendicular to the inspected tangent plane of the pipe surface. The transducer clamping device has three moving parts. A water film within a setting range of 25 mm in thickness is reserved to keep the transducer away from the workpiece and to protect the transducer from damaging when an uneven surface is encountered. The clamping adjustment device can adjust the angle of the transducer adaptively for any diameter within the range of 73–140 mm. A cavity is formed when water is added to ensure the transducer and the workpiece completely filled with water and to guarantee scanning accuracy.

The aforesaid signal processing and imaging algorithms were integrated into a software. The designed graphical user interface (GUI) is shown in Fig. 4. The software for visualization analysis of ultrasonic detection was developed in MATLAB. It can realize the analysis of ultrasonic detection signal and the reconstruction of the pore structure of the high-temperature self-propagating coating on the

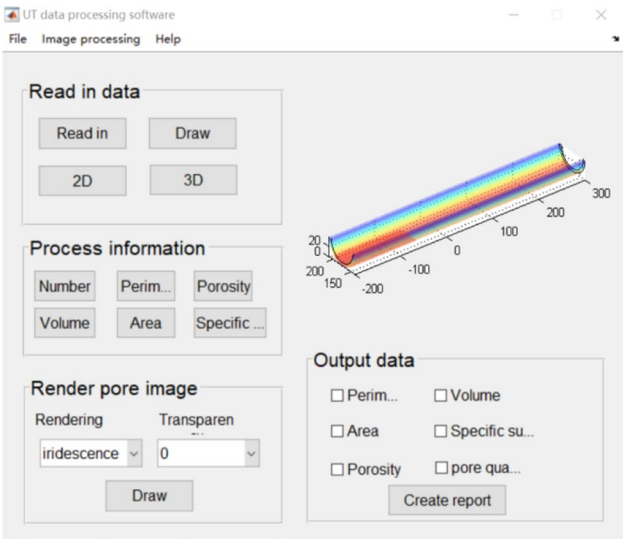

Fig. 4 The software GUI display of a pipe specimen

inner wall of parts, and quantitatively measure a series of characteristic parameters such as porosity, pore quantity, volume and area, morphology, spatial distribution, and specific surface area of the coating.

2.2 Materials and the test object

In this research, we consider a ceramic-lined steel composite pipe as the tested object of the typical inhomogeneous multi-layered pipe. The preparation mechanism of this kind of pipe is the thermit reaction [10, 11]. Finally, the structural composition is shown in Fig. 5.

The ceramic-lined steel composite pipe with an external diameter of 73.02 mm and its pre-remanufactured steel-matrix pipe are most commonly used in oil and gas industry. The real products of this specification are shown in Fig. 6. The dimensions of the most commonly used ceramic-lined steel composite pipes are listed in Table 1 [12].

To detect the deep inner hole of remanufactured pipe parts, artificial defects should be preproduced on the inner wall. At present, there is limited relevant work on alumina

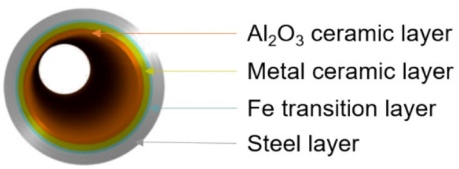

Fig. 5 A diagram of the structural composition of ceramic-lined steel composite pipe

Fig. 6 A real product of ceramic-lined steel composite pipe

ceramic materials available for reference. For layered pipe pieces, the main difficulties are as follows:

1. The characteristics of the ceramic coating including high hardness, brittleness, electrical insulation and non-ferromagnetism make traditional processing methods hard to implement and likely to damage the lining layer of the inner wall.
2. The inner hole is too deep for the processing equipment to reach.
3. UT requires that the artificial pore defects should be approximately flat-bottom to reduce diffuse reflection of acoustic waves at the location of round angles and the arc of the bottom surface which will weaken the signal.

Thus, it is difficult to fulfil the preproduction work via general grinding and other processing methods. Hanon et al. [13] and Kacar et al. [14] used Nd:YAG pulsed laser for micromachining plate ceramic materials. In our work, laser cutting technology was also used to cut pipe parts along the axial section after the remanufacturing of 500 mm in length, and laser drilling technology was used to process the hole defects in its inner wall. The equipment used was Han's Laser G4020F Optical Fiber Laser cutting machine. The hole diameter ranges within 3–9 mm with a designed depth of about 1.5 mm, and the ceramic was not cut through. The hole edge spacing was 40 mm. The preparation process is shown in Fig. 7. Results show good machining effect and the ceramic at cutting edge is complete without extensive shedding. The pores are of good conformality. After punching on the groove of the half part, two half parts were glued together to restore the integrated tube.

2.3 UT and signal processing

A set of ultrasonic digital signal and image processing algorithm is designed aiming at UT of pipe parts, as is shown in Fig. 8. The technical requirements to be realized can be summarized as follows: (1) the bonding quality

Table 1 Dimensions of a typical composite pipe

Steel pattern no.	Outside diameter (OD) (mm)	OD tolerance mm	Steel wall thickness mm	Wall thickness deviation	Steel-inside diameter (mm)	Lining thickness (mm)	Ceramic-lining inside diameter (mm)
J55	73.02	±0.79	5.51	−12.5%	62.0	2.5	57.0

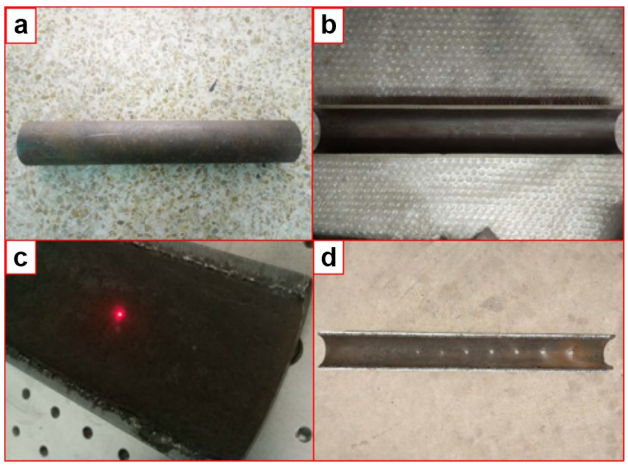

Fig. 7 Preparation process of ceramic-lined composite steel tubes with prefabricated artificial defects: **a** a 500 mm long remanufactured pipe specimen, **b** a laser cut specimen, **c** laser drilling, **d** a specimen with artificial defects

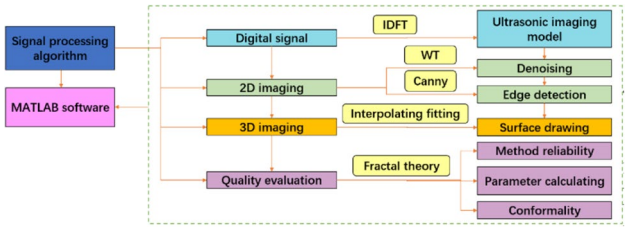

Fig. 8 A flow chart of the signal processing algorithm

assessment of sampling points and calculation of the overall area ratio of poor-bonding areas; (2) to conduct qualitative and quantitative detection of defects such as inner wall holes, cracks, coating thickness reduction and debonding; (3) 3D volume rendering measurement and analysis to get intuitive images.

Algorithms regarding the fractal theory is mentioned in previous work [15].

2.3.1 Digital scan transformation

The digital scan converter (DSC) establishes a mapping relationship between the ultrasonic scan and the display scan. An ultrasonic transducer receives 3D echo signals and converts them into 3D digital array signals. Through data acquisition and analysis software, the RGB image in the form of rectangular coordinate system is displayed on the monitor data for subsequent processing [16].

2.3.2 Surface fitting based on 2D cubic convolution interpolation

In terms of irregular distribution of discrete sampling points on the grid, it is necessary to conduct data gridding. With 2D interpolation, the interval of 3D spatial coordinate data can be equal, and then regular grid data are generated for computer processing. Cubic convolution interpolation (CCI) is one of the most commonly used 2D interpolation methods. The kernel function of CCI is composed of piecewise cubic functions on four intervals, considering the influence of direct and indirect neighboring points [17, 18].

Therefore, this work constructs a quadric surface fitting algorithm for spatial discrete points based on cubic convolution interpolation. The key steps are as follows:

1. To define X and Y axis interpolation data points respectively according to the actual situation;
2. To generate N_x and N_y interpolation points respectively at equal intervals between the maximum and minimum values of the original X and Y data;
3. To perform cubic convolution interpolation.

2.3.3 Quantitative calculation

According to the reconstructed surface image, 3D reconstruction of volume data of the pipe body and defects can be performed, and then the location, size and depth of the target defects can be measured and calculated. The quantitative calculation procedure is designed as follows:

1. To import dimension parameters of the pipe and draw the pipe body;
2. To draw the curved surface;
3. To generate cylinder data with radius (r) and height (h);
4. To adjust color and transparency;
5. To calculate the surface area;
6. To measure defect locations and sizes;
7. To calculate the defect surface area and depth.

3 Results and discussion

3.1 Edge detection

The canny operator is employed on the C- and TOF-scan images of an artificially marked test-piece, as is shown in Fig. 9. From the processing results, it can be seen that the image with dual-threshold segmentation and gradient segmentation can effectively detect the artificial markers and edges of thickness reduction areas.

The same algorithms were performed on the specimen with seven artificial pores which were all clearly visible via gradient edge segmentation, as shown in Fig. 10.

Ultrasonic scanning method is theoretically feasible for NDT of multi-layered composite materials. Experimental results have demonstrated the effectiveness of the method and the equipment for visual detection of remanufactured pipe parts.

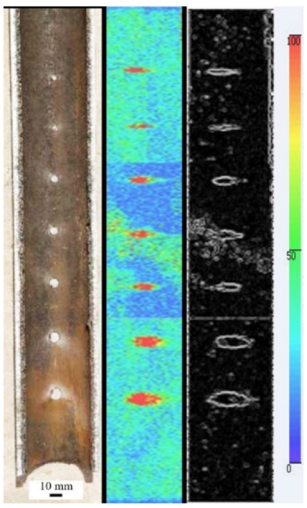

Fig. 10 The C-scan image and its gradient edge segmentation result of the whole test-piece

3.2 3D volume data reconstruction

The 3D reconstruction algorithm enables defects to be imaged proportionately to their actual depth on the inner wall of the pipe model. Local scanning was done on artificial pores with a diameter of 8 mm and 9 mm on a test specimen for further surface rendering, target defect extraction and 3D imaging.

3.2.1 Surface rendering

Digital signals captured by the ultrasonic scanning device were converted into a 3D view and a C-scan image via CCI algorithm. As is shown in Fig. 11c, the blue areas represent thickness reduction. The obvious dual-pore structure can be seen in the region of interest. The position and depth of the pores were calculated from the coordinate, and then the remaining wall thickness were obtained.

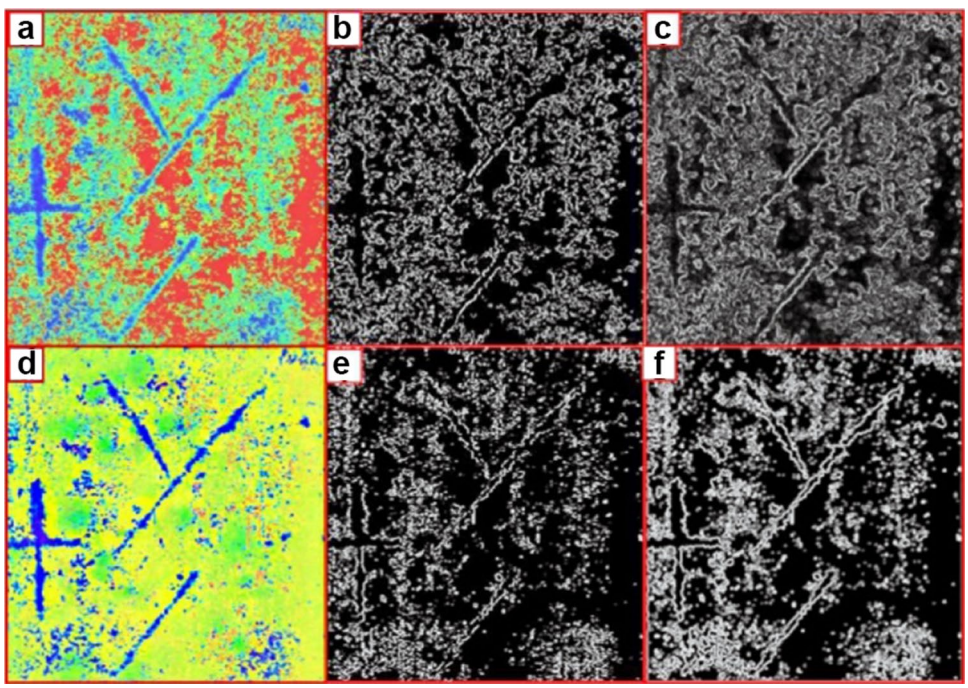

Fig. 9 Scanning images of the artificially marked test-piece **a** C-scan image, **b** dual threshold segmentation of C-scan image, **c** gradient segmentation of C-scan image, **d** TOF, **e** dual threshold segmentation of TOF-scan image, **f** gradient segmentation of TOF-scan image

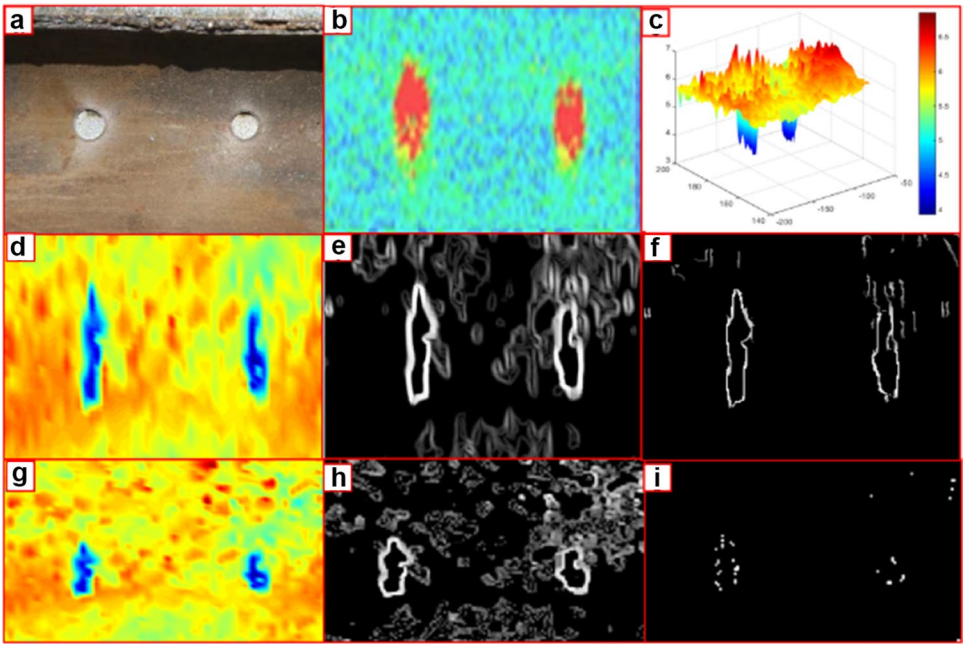

Fig. 11 The dual pores on the ceramic-lined specimen **a** photo of real object, **b** C-scan image, **c** digital signal reconstructed surface, **d** digital signal reconstructed 2D RGB image, **e** gradient segmentation of 2D image, **f** dual-threshold segmentation of 2D image, **g** corrected 2D digital signal reconstruction RGB images, **h** corrected 2D image gradient segmentation, **i** corrected 2D image dual-threshold segmentation

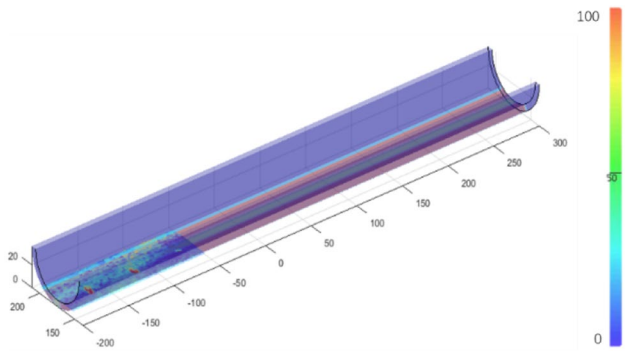

Fig. 12 A 3D reconstruction surface with target defects

Fig. 13 Real topography of the artificial hole

3.2.2 Target defect extraction

The canny operator is used in the 2D planform of Fig. 11b, c for gradient and dual-threshold segmentation, considering the dual-pore as the target defect.

3.2.3 3D imaging

To get consistent C-scan color code, color inversion was set for the reconstructed surface, namely using red regions to indicate local thickness reduction. The 2D RGB diagram of the reconstructed surface after color reversal was superimposed with the 3D image of the tube body to obtain an overall 3D view with the location and basic morphology of the target defects, as is shown in Fig. 12. The position and size were calculated via the software from coordinates.

3.3 System verification

3.3.1 Calculation of defect characteristic parameters and error estimation

To verify the quantitative detection effect, the artificial hole defect specimens were scanned locally. The area with designed apertures of 8 mm and 9 mm respectively and a designed depth of 1.5 mm was selected. The remaining wall thickness at the artificial hole position was measured with the screw micrometer. The diameter D and depth H of the artificial hole defects were calculated quantitatively using the designed software. The surface topography of the artificial pore is shown in Fig. 13.

The relative error limit between the calculated value and the measured value is defined as

$$\varepsilon_r^* = \frac{\varepsilon^*}{|x^*|} = \frac{|x^* - x|}{|x^*|}$$

Table 2 Characteristic parameters of manual pores

	Diameter of pore 1 (D_1)	Depth of pore 1 (H_1)	Residual wall thickness of pore 1 (R_1)	Diameter of pore 2 (D_2)	Depth of pore 2 (H_2)	Residual wall thickness of pore 2 (R_2)
Designed value (mm)	9	1.5	6.51	8	1.5	6.51
Measured value (mm)	9.015	1.514	4.996	8.120	1.521	4.989
Calculated value (mm)	9.116	1.476	5.034	7.930	1.590	4.920
Relative error (%)	1.1079	2.5745	0.7549	2.3960	4.3396	1.4024

where ε_r^* is the relative error limit, ε^* is the absolute error, x is the measured value and x^* is the calculated value.

As can be concluded from Table 2, the relative error limit between the calculated value and the measured value is lower than 5% in these cases.

3.3.2 Image size reduction and correction

Improvement of 2D reconstruction algorithm for ultrasonic 3D array was applied, as the reductive degree of the defect shape and size was relatively low when the surface was drawn. The x and y coordinates were adjusted and corrected so that the x/y ratio was closer to the real value. Figure 11g–i show a series of images with modifications added.

4 Conclusion

This work focuses on visualized NDT for corrosion failure assessment of metal substrate pipe parts and preparation of ceramic-lined remanufactured pipe parts in the process of onsite quality inspection. Ultrasonic signal processing and imaging algorithms for composite pipes were constructed and the analysis of UT visualization software was developed in MATLAB. The visualization device can be used to detect hidden safety problems of the tube parts in service, which will provide a technical support for NDT of deep hole parts before and after remanufacturing.

A data processing software developed in MATLAB can be used to achieve a variety of digital signal processing functions: IDFT was employed for ultrasonic data acquisition and imaging. The image noise was reduced with WT. The canny operator was used for image segmentation and edge detection. CCI was used to realize surface fitting and 3D data reconstruction. Finally, coating defects were characterized and calculated quantitatively.

Combined with a special UT device for visual ultrasonic detection of deep hole parts, the whole software and hardware system was used for detection and verification of artificial defects. The volume data reconstruction algorithm can realize the extraction of target defects and 3D imaging of the detected object. The relative error limit of the calculated value of the diameter and depth of the artificial hole defects was less than 5%. The detection method, system equipment and algorithm program designed in this work are of practical application value with strong feasibility and applicability.

Though defects in multi-layered pipes have been visualized and the flaw size error has been estimated in this work, the probability of detection (POD) and some other performance evaluation indexes still require further study and the integrated hardware and software system should also be applied in field tests for performance verification.

Acknowledgements The authors would like to thank financial supports from the National Natural Science Foundation of China (51675533, 51701238). The reviewers providing valuable advice and comments on the revision of this paper are also appreciated.

Compliance with ethical standards

Conflict of interest The authors declare that they have no conflict of interest.

References

1. Skjelvareid MH, Tomas O, Yngve B (2012) Three-dimensional ultrasonic imaging in multilayered media. In: AIP conference proceedings 1433, AIP No. 1
2. Wu S et al (2015) Synthetic aperture imaging for multilayer cylindrical object using an exterior rotating transducer. Rev Sci Instrum 86(8):083703
3. Kolkoori S, Hoehne C, Prager J et al (2014) Quantitative evaluation of ultrasonic C-scan image in acoustically homogeneous and layered anisotropic materials using three dimensional ray tracing method. Ultrasonics 54:551–562
4. Iyer S, Sinha SK, Pedrick MK et al (2012) Evaluation of ultrasonic inspection and imaging systems for concrete pipes. Autom Constr 22:149–164
5. Yang C, Qin K, Li Y (2014) Real-time ultrasonic imaging for multilayered objects with synthetic aperture focusing technique. In: Proceedings of 2014 IEEE international instrumentation and measurement technology conference (I2MTC), pp 561–566
6. Cui W, Qin K (2018) Real-time total focusing method imaging for ultrasonic inspection of three-dimensional multilayered media. In: 2018 IEEE international conference on acoustics, speech and signal processing (ICASSP), pp 6513–6517
7. Nagamune A, Nishifuji K, Iizuka Y (1995) Ultrasonic inspection system for tubular products using real-time digital signal processing. NDT&E Int 28:303–306

8. Kažys RJ, Tumšys O, Pagodinas D (2008) A new ultrasonic technique for detection and location of defects in three-layer plastic pipes with a reinforced internal layer. Ultragarsas 63(3):19–27
9. Asmani M et al (2001) Influence of porosity on Young's modulus and Poisson's ratio in alumina ceramics. J Eur Ceram Soc 21(8):1081–1086
10. An J, Zhao J, Su Z et al (2015) Preparation, infrared emissivity and electromagnetic property of SnFeO (x = 0, 0.03, 0.06, and 0.09) solid solution powders by coprecipitation method. Arab J Sci Eng 40:10
11. Mahmoodian R, Rahbari RG, Hamdi M et al (2013) The effects of an unexpected ceramic coating phase at the head of a pipe on joining and postprocessing of a ceramic-lined composite pipe. JOM 65:80–85
12. Institute of Metallurgical Industry Information Standards (2000) YB/T 176-2000 ceramic-lined composite steel tubes. China Standard Press, Beijing
13. Hanon MM, Akman E, Oztoprak BG et al (2012) Experimental and theoretical investigation of the drilling of alumina ceramic using Nd: YAG pulsed laser. Opt Laser Technol 44:913–922
14. Kacar E, Mutlu M, Akman E et al (2009) Characterization of the drilling alumina ceramic using Nd: YAG pulsed laser. J Mater Process Technol 209:2008–2014
15. Zhu Y, Wei SC, Dong YC et al (2017) The study of a novel ultrasonic A-scan signal processing method based on fractal theory. Mod Phys Lett B 31:1740027
16. He W, Wang P, Luo XH (2014) Imaging principles and system design of digital ultrasound. Science Press, Beijing
17. Guolong TRW (2006) Application of cubic convolution interpolation in synthetic aperture radiometer. Electron Meas Technol 29:103–105
18. Keys R (1981) Cubic convolution interpolation for digital image processing. IEEE Trans Acoust Speech Signal Process 29(6):1153–1160